

ATF CO₂ Laser Upgrade Plan

Introduction

The ATF Mission

Brookhaven National Laboratory's (BNL's) Accelerator Test Facility (ATF) was established over a quarter of a century ago by two visionaries of accelerator science, Robert Palmer and Claudio Pellegrini. From its inception, it has operated as a users' facility through a proposal-driven, program-committee-reviewed process. It offers state-of-the-art tools in electron-beams and synchronized laser beams providing unique opportunities for developing applications utilizing fundamental accelerator- and laser-science.

Over the last two decades, the Accelerator Test Facility (ATF) has become the destination for national and international scientists from academia, small businesses and National Laboratories doing their research in advanced accelerators and radiation sources. Overall, hundreds of researchers from a wide spectrum of institutions worldwide have conducted ground-breaking experiments at the ATF with the help and participation of members of our staff. The ATF serves as a training ground for post-docs and graduate students. The science and technology engendered at the ATF are documented by numerous publications that are frequently cited.

A varied plethora of user experiments, carried out over the entirety of the ATF's history, falls into four subject areas:

- Accelerator-beam physics
- Particle sources and beam instrumentation
- Novel acceleration techniques
- Novel radiation sources

Our Capabilities due to the Combination of a High-Brightness e-Beam and Terawatt CO₂ Laser

The ATF offers a unique platform for conducting state-of-art experiments that is empowered by the combination of its key components: High-brightness electron- and laser- beams. **Figure 1** is a block-diagram of the ATF with its 80-MeV RF linac and a terawatt CO₂ laser, linked and synchronized at the picosecond-level with a common Nd:YAG laser that simultaneously drives the photocathode RF gun and slices a picosecond 10- μ m laser pulse for seeding the CO₂ laser's amplifier chain.

A CO₂ gas laser, with its 10-12-fold longer wavelength than that of ultra-intense solid-state lasers (e.g., Titanium-sapphire lasers), which are tools for strong-field physics research, offers several distinctive features that facilitate certain classes of experiments. With it, researchers can exploit the following added benefits:

- A. Favorable scaling of accelerating structures, and better electron phasing into the field,
- B. Stronger ponderomotive effects at the same laser intensity,
- C. Tenfold more photons per Joule of laser energy, and,
- D. A hundred-fold, lower critical plasma density.

These features justify the logic that drove to the initial selection of a CO₂ laser for the facility, as well as the motivation for user experiments. This choice was prudent as proved by the resounding success of our users' diverse experimental program in which the ATF achieved many "firsts": Inverse-Cherenkov laser acceleration; high-gain harmonic generation (HGHG) FEL; plasma channeling of a high-power CO₂ laser; laser-driven ion acceleration;

acceleration/focusing phasing in Plasma Wakefield Acceleration (PWFA); high-gradient Inverse Free Electron Laser (IFEL) accelerator; micro-bunching from IFEL; Particle Acceleration by Stimulated Emission of Radiation (PASER); nonlinear Thompson scattering; and, the first staging of laser accelerators (two IFEL accelerators in series).

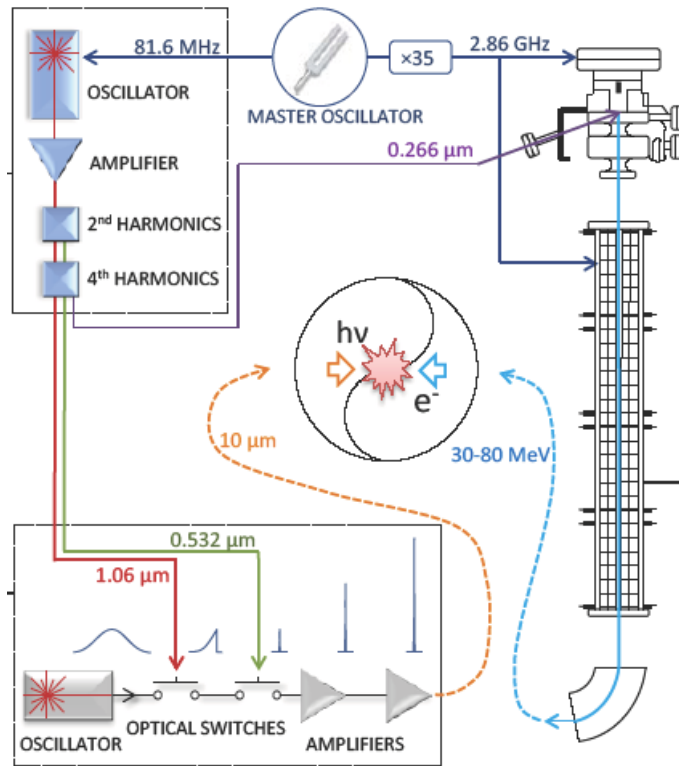


Figure 1. ATF architecture.

From its very inception, the ATF steadfastly has continued its quest to offer new opportunities for user experiments by elevating the CO₂ laser's peak power. The diagram in **Figure 2** represents a historical perspective of the evolution of the ATF's laser over the last 20 years: it shows the dramatic increase in power of nearly three orders-of-magnitude that we have realized from early years to the present. Every step up in the laser's power enabled a new series of user experiments, as is illustrated. These accomplishments simultaneously build up the ATF's legacy in research on advanced accelerators and on radiation sources, thereby underscoring the advantages of successfully exploiting the long-wavelength laser driver in the ATF users' experiments.

Similar advantages will be gained at the even higher laser powers we plan to deliver, enabled by further upgrades discussed below. The ultra-high power IR laser will afford ATF's users a first-time opportunity to explore *wavelength scaling* of strong-field physics phenomena at a laser strength parameter $a_0=10$, and wavelength $\lambda=10 \mu m$.

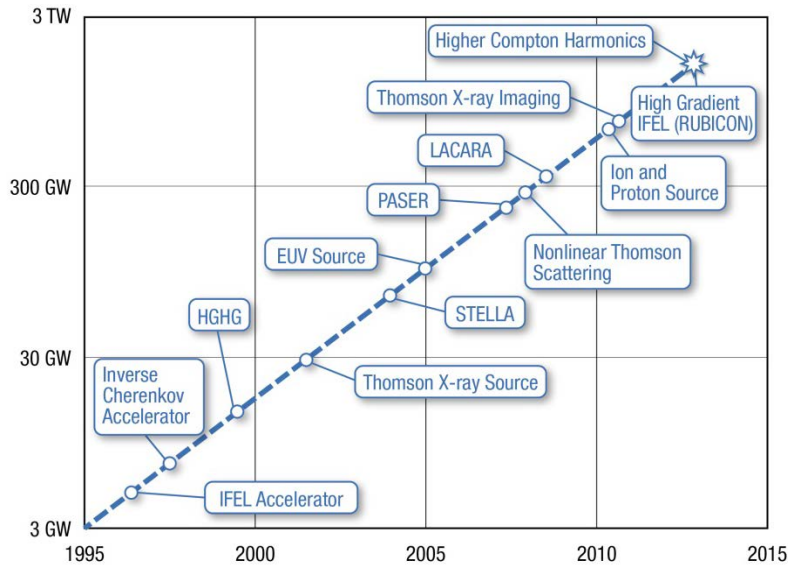


Figure 2. History of ATF user experiments enabled by our continuing upgrades of CO₂ laser power.

The 100 TW CO₂ Laser Power Upgrade

The evolution of the ATF’s picosecond CO₂ laser up to this time was centered on significantly shortening the pulse’s duration (from 200 ps to 5ps) and increasing its energy (from 200 mJ to 5 J). We achieved this via building up the system, adding components and features that qualify as “evolutionary” upgrades. Further progress towards yet much higher peak powers will require our devising a next-generation ultra-fast CO₂ laser technology via implementing “revolutionary” methods never employed previously with gas IR lasers. Our plan includes four major innovations: All-solid- state, femtosecond, optical parametric amplifier front end; chirped pulse amplification; self-chirping and femtosecond compression; using CO₂ isotopes in amplifiers. These developments parallel similar revolutionary betterments made years ago in solid-state laser technology wherein “ultra-fast” is the terminology now applied to lasers of 100 fs and shorter pulse length. Although “next-generation ultra-fast CO₂ lasers” signify lasers with pulses shorter than 1 ps, the same “ultra-fast” terminology is fully applicable and justified in view of the small number of laser cycles (30 or less) within the pulse.

The upgrade of the ATF’s CO₂ laser undoubtedly will provide new research program opportunities at BNL. By offering a unique, compact and powerful laser, new scientific missions will be enabled including the following ones: Ion acceleration of the radiotherapy relevance; creation of ultra-bright sources of monochromatic X-rays through inverse Compton scattering; high-luminosity laser wakefield acceleration of electrons, and other strong-field applications that complement cutting-edge projects conducted or planned with the most powerful solid state lasers worldwide.

Detailed Plan

Our upgrade of the ATF’s CO₂ laser system to 100 TW level will be achieved through three main thrusts:

- 1) Adding stages to the laser’s amplification chain.

- 2) Applying known ultra-fast solid-state laser techniques towards the next-generation CO₂ laser technology, by
 - a) implementing the Chirped Pulse Amplification (CPA) technique in the CO₂ laser, and,
 - b) installing a high-power Optical Parametric Amplifier (OPA).
- 3) Implementing femtosecond-pulse compression.

The program also entails the enhancement of many auxiliary systems, including transport, computer controls, supply lines, and controlled clean-room environment.

Optical Parametric Amplifier (OPA)

After thorough consideration, we selected and currently are commissioning a new front end of the ATF CO₂ laser system, i.e., an optical parametric amplifier(OPA) based on nonlinear mixing crystals pumped with a Ti-sapphire laser.

This all-solid-state seed-pulse generator manufactured by Quantronix Co. produces 35- μ J, 350-fs (FWHM), 10- μ m pulses. The natural bandwidth of the 350-fs injection pulse is about threefold broader than that of a CO₂ amplification band. Hence, the pulse spectrum will shrink upon amplification, with a simultaneous rise in its duration to 1.5-2 ps. This still affords us a two-to-three-fold improvement over the current minimum duration of the pulse which is limited at \sim 5 ps by the speed of optical switches used for generating the injection pulse. Another improvement follows from the fact that the broadband injection pulse will extract excitation energy simultaneously from a manifold (\sim 15) of rotational sub-levels on the upper vibrational laser level, compared to only \sim 3 rotational sub-levels interacting with a 5-ps pulse. We estimate attaining an order-of-magnitude higher total gain in the peak power due to pulse shortening (a factor of 3) and better extraction of energy (again a factor of 3).

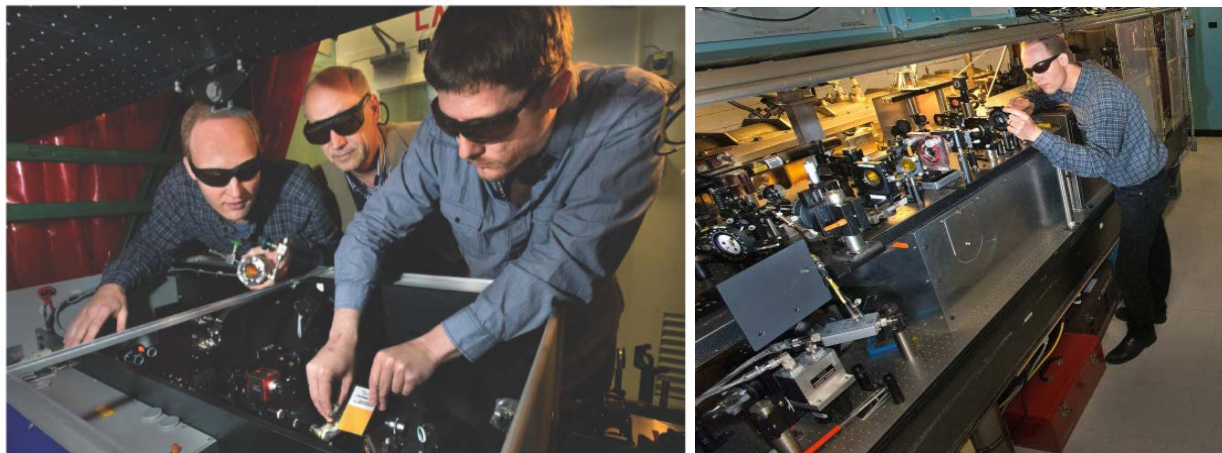


Figure 3. Compact solid-state femtosecond OPA (left) will replace the present-day seed-pulse generation front-end (right).

Figure 4 shows the layout of the 5-TW 10-micron laser system after installing and implementing our new, seed-pulse OPA generator.

A future upgrade of the seed-pulse generator that we are considering will implement an additional OPA stage that will be pumped by a solid-state laser. It will be built upon the proven architecture of the current Quantronix seed system. Commercial large-area crystals supporting pump intensities high enough to achieve 1 mJ output are available; however, an integrated high-energy OPA system at this level is not. Therefore, we plan to integrate the optical components in-house.

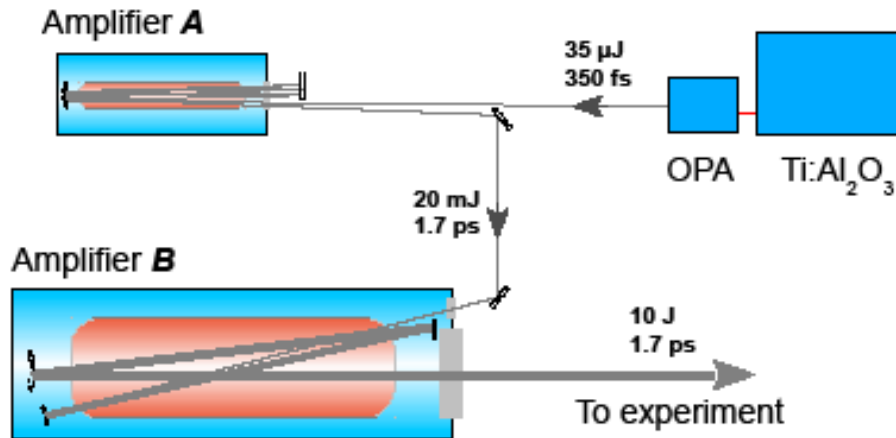


Figure 4. Layout of the ATF's 10-micron laser system after implementing the all-solid-state seed-pulse generator.

Amplifier chain

We will build a new amplifier chain starting from the existing ATF CO₂ laser system. The expansion of the amplifier chain, aimed primarily at boosting the laser energy, will encompass the following three steps:

Step 1. We will extract more energy from the initial regenerative amplification stage. Presently, this amplification stage (SDI Co., UV-pre-ionized discharge, 10-atm, 12-mm aperture, isotopic regenerative amplifier) is limited to ~5 mJ output energy. By augmenting this stage with a larger-aperture CO₂ amplifier (~30 mm), we will greatly increase the output, to 30-50 mJ.

To accomplish this step, we will purchase another SDI laser amplifier custom-developed to our specified requirements (see **Figure 5**).

Step 2. We will modify an existing multi-pass, 10-cm aperture, x-ray pre-ionized, CO₂ laser amplifier manufactured by Optoel Ltd. to have fewer passes but with simultaneous expansion of the laser beam's aperture at the early passes. Because of the larger energy input from the initial amplification stage, the multi-pass amplifier will attain the same energy per beam area, per unit bandwidth. However, because the expanded beams cover a larger active area, the broader spectrum (ensured by the OPA), and the longer pulses (due to CPA stretching as detailed below), the extraction energy from the Optoel amplifier will be much higher than that in the current system, reaching 30-45 J compared with <10 J now, that is a remarkable improvement.



Figure 5. Commercial 10-atm CO₂ laser manufactured by SDI Ltd. (RSA)

Step 3. We will build an additional final amplifier, according to the acquired blueprints (see fragments of this laser illustrated by **Figure 6**), with only one or two amplification passes and efficient energy extraction from the entire active area. The expected output energy will be above 100 J.

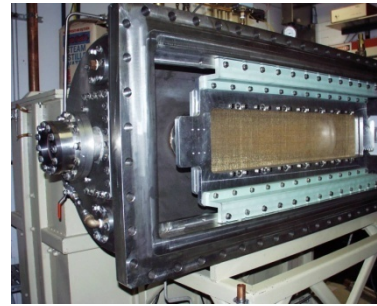
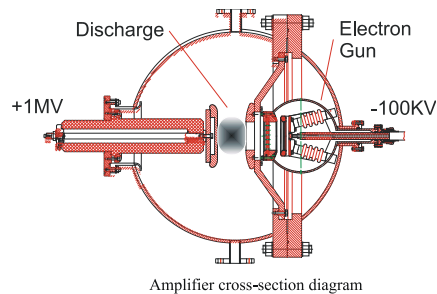


Figure 6. New Laser amplifier to be built from blueprints available from previous Optoel contract. Right picture shows essential part of the laser's active head depicted at the left.

Chirped Pulse Amplification (CPA)

The invention of CPA was a dramatic breakthrough in the field of solid-state laser technology, and we expect that its effect on gas lasers will be equally invaluable. Although the nonlinear indices of the gaseous active media are smaller than those of the solid-state ones by several orders-of-magnitude, the presence of transmitting optics and long beam-paths make the nonlinear effects (Kerr lensing, self-phase modulation) also a problem for high-peak-power CO₂ lasers. Resolving it is vital for making further progress in increasing the peak power. For example, a recent reconfiguration of the ATF's regenerative amplifier, wherein we replaced an intra-cavity Pockels-cell switch based on a 5-cm CdTe crystal with a 500- μ m Ge semiconductor switch, satisfactorily raised the energy of the amplifier output from 1 mJ to ~10 mJ. In the next-generation CO₂ lasers, where we aim to reach significantly higher peak intensities, we consider that the CPA is the obvious way to go.

The high-energy extraction from the active medium, described above, and its transmission through the amplifier windows is possible provided that the CO₂ seed pulse stretches to 100-200 ps with diffraction gratings. We plan to introduce a stretcher after the OPA or, alternatively,

another early amplification stage. **Figure 7** shows the principle optical design of a stretcher and a compressor for CPA.

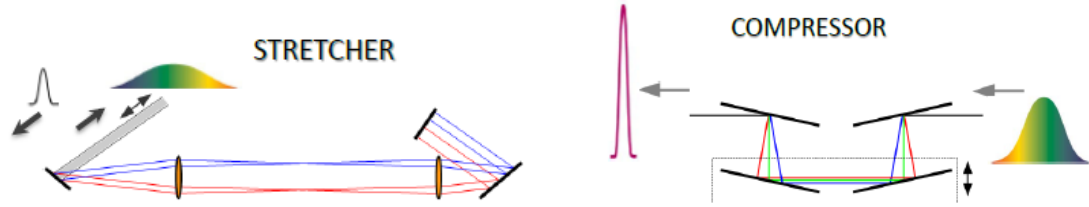


Figure 7. Principle optical diagram of CPA components with picosecond pulse stretching and compression using diffraction gratings.

The diffraction grating compressor will be housed in a vacuum chamber, placed before the final focusing parabola at the applicable experiment location (ion acceleration or laser/e-beam interaction point). The technical characteristics of the CPA apparatus are compiled in **Table 1**.

Table 1. Technical parameters of the CPA apparatus

Grating line density	75 mm ⁻¹
Grating blaze angle	22°
Grating angular dispersion @ 10 μm	0.081 rad/μm
Stretcher grating:	58×58 mm ² , Al on Zerodur substrate, replica
Stretcher configuration	Folded, single grating
Design stretching factor	680 ps/μm
Example stretching	1 ps → 100 ps (FWHM, bandwidth-limited Gaussian pulse)
Compressor gratings:	Stage 1 (5-10 TW): 165×220 mm ² , Al on Cu substrate, replica Stage 2 (100 TW): 320×320 mm ² , bare Al, master
Compressor configuration	Unfolded, 4-grating
Compressor vacuum rating	E-8 Torr

After compressing the pulse back to ~3 ps, the combination of CPA with the improved energy output from the amplifier chain will produce 30-50 TW peak laser power. Our projection is supported by simulations presented in **Figure 8**. To our knowledge, this will be the first-ever simulation of the CO₂ CPA regime. The simulations demonstrate that despite noticeable narrowing and modulation of the laser pulse's spectrum during amplification, efficient recompression is still attainable.

Femtosecond pulse compression

Frequency chirping, induced by the Kerr effect via transmitting the laser beam through a Xenon gas-pipe, supports additional compression of the pulse past the diffraction gratings. The effect has been previously demonstrated on a small scale with a CO₂ laser and is well characterized through simulations that verify the likelihood of compressing 2 ps CO₂ laser pulses down to 0.5 ps with high conversion-efficiency (see **Figure 9**). We expect to realize a rise in the final peak power from 30-50 TW to 100 TW upon our implementation of this process.

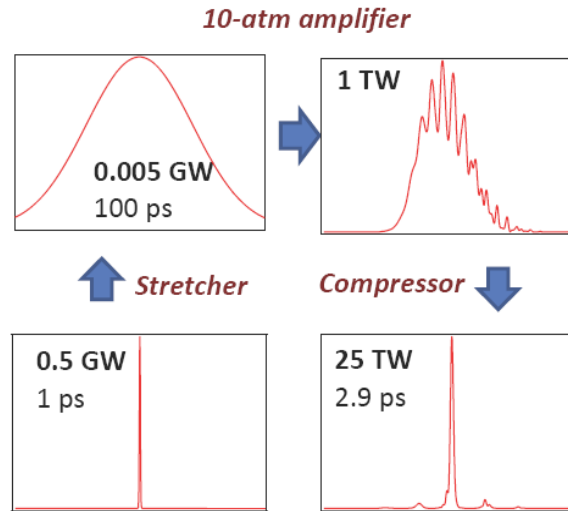


Figure 8. Simulation of dynamic changes in the laser pulse through a stretcher-amplifier-compressor chain in a CPA CO₂ laser.

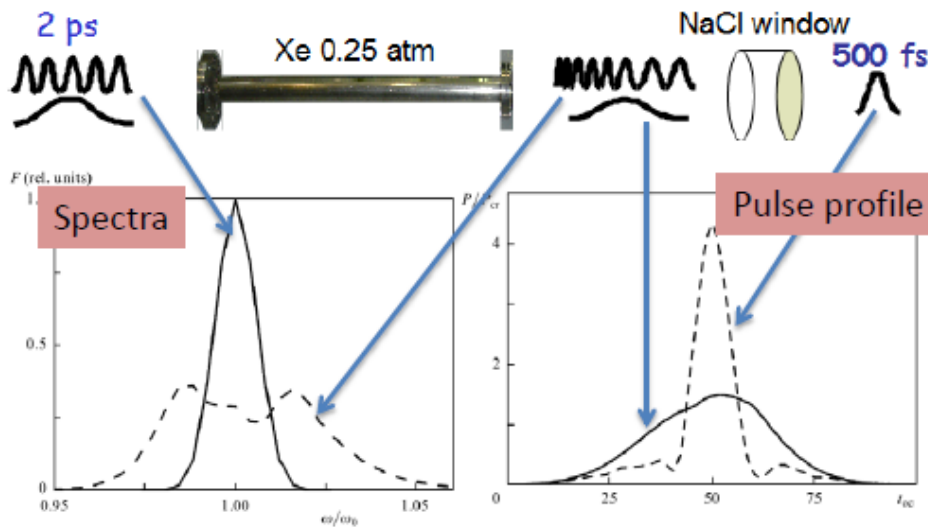


Figure 9. Principle diagram for femtosecond pulse compression method

The principle optical layout for the 100 TW CO₂ laser system is shown in **Figure 10**.

100 TW Implementation Plan

The ATF CO₂ laser upgrade to 100 TW peak power is being planned independently from this proposal, under funding from BNL's Program Development (see **Table 2**).

Although we already have initiated work on certain elements of the CO₂ laser power upgrade, and will continue it within the present ATF envelope in Bldg. 820, the full advantages of this upgrade will be difficult to realize due to cumbersome space restrictions. Still more critical for our success is the availability of radiation-shielded space for undertaking experiments with ultra-

high power laser beams: Up to 200 MeV proton- beam energies can be expected after focusing the 100-TW CO₂ laser beam onto a hydrogen jet. Setting up Ion Acceleration experiments and applied Radiation Biology tests requires a dedicated radiation-shielded hall.

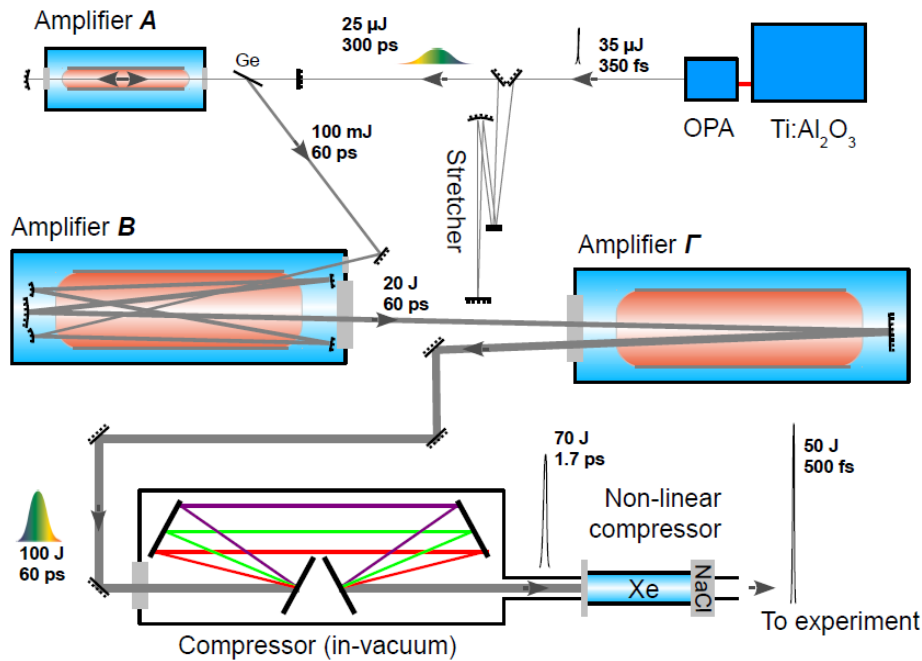


Figure 10. Principle diagram of the ATF CO₂ laser system after the proposed 100 TW power upgrade.

Table 2. Tentative 100 TW CO₂ laser program schedule

ID	Task Name	2014				2015				2016				2017
		Qtr 1	Qtr 2	Qtr 3	Qtr 4	Qtr 1	Qtr 2	Qtr 3	Qtr 4	Qtr 1	Qtr 2	Qtr 3	Qtr 4	Qtr 1
1	Final amplifier	\$900,000.00												
2	Isotopic preamplifier	\$660,000.00												
3	Stretcher and compressor					\$180,000.00								
4	OPA					\$160,000.00								
5	Auxiliary components									\$200,000.00				

We plan to complete the laser upgrade after the proposed ATF relocation to Bldg. 912 that will assure adequate space and sufficient infrastructure for accommodating the laser as well as its efficient utilization for user experiments. Advantageously, this expansion includes our ability to offer a safe working environment by separating and isolating the operator control station, with its sensitive computers and electronics, and a low-power front end from final high-energy amplifiers, with their potential ionizing radiation and Electro-Magnetic Pulse (EMP). Simultaneously, the ATF operators and users will benefit from a bigger control room that will accommodate a control station for remotely operating the Ion Acceleration and biological experiments. The layout of the future CO₂ laser rooms is illustrated in **Figure 11**.

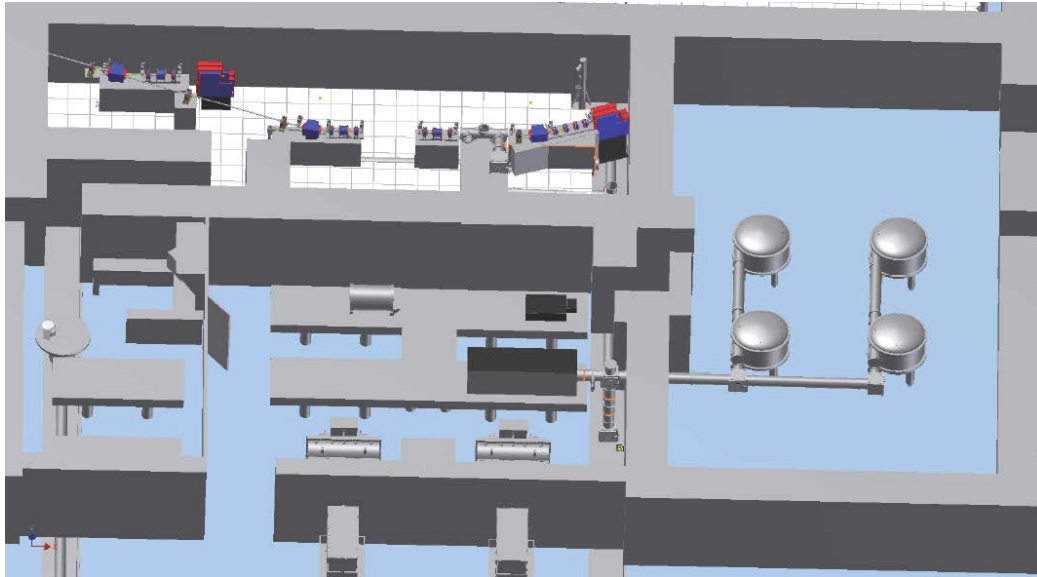


Figure 11. Layout of CO₂ laser rooms with experimental hall dedicated to laser/e-beam experiments (to the top) and “laser only” experiments (to the right) in bldg. 912

Adjacent to the CO₂ rooms will be Exp. Hall #2 with electron beam lines and experimental chambers for laser/e-beam interaction experiments. Bringing ultra-high power laser beams to the electron beam lines will secure our role in the next-generation of laser/e-beam interaction experiments, such as Inverse Compton Scattering and Laser Wakefield Electron Acceleration.

Exp. Hall #4, with its radiation shielding capability, will be dedicated to Ion Acceleration experiments encompassing with biological test stands, THz- and HHG- radiation sources; and the space for other potential “laser-only” user experiments.

The 100 TW laser beam generated at the final CPA compression station will be distributed with kinematic mirrors to EH#2 and EH#4. This requires our employing big-aperture (up to 10”) laser optics enclosed within large-diameter high-vacuum transport lines and optical setup chambers. Maintaining high vacuum in the transport lines is essential, not only to avoid degradation of the optics and self-focusing and other detrimental effects upon propagation of the high-power beam through the air, but also to avoid any refractive optics (windows) in the way of the beam that could distort it due to the Kerr effect and optical breakdown.

Laser safety interlocks and personnel-warning equipment will be installed at the requisite areas. Other auxiliary components include clean enclosures to accommodate the expansion of the laser system, new diagnostics for high-power beams, in-vacuum optical transport lines, gas- and vacuum-services, and computer controls.

The laser upgrade strategy anticipates its flexible adaptation to the facility’s needs for ensuring minimally interrupted service to user projects. Such a strategy is applicable since the schedule we have set for the laser upgrade anticipates our procuring new laser components that, taken separately, can perform at the level of the present ATF CO₂ laser system. This way, all experiments conducted at the old ATF location may be restarted almost immediately at the new location after its commissioning is finished. Upon relocating the laser components from ATF and reinstalling them, the laser upgrade project will be completed to the 100 TW level.

Science Motivation for 100 TW upgrade

The justification for engaging into the development of new ultra-fast CO₂ laser technology rests on the same aforementioned arguments that have prioritized an IR laser for several classes of experiments throughout the ATF's history. Integration of the ultra-high power IR laser will afford ATF's users with unique opportunities to explore *wavelength scaling* of strong-field physics phenomena at a laser strength parameter $a_0=10$, and wavelength $\lambda=10 \mu m$. Opportunities for scientific breakthroughs abound in different areas of research, including the following ones:

- Ion Acceleration to the 200-MeV level, as is needed for medical applications;
- Laser Wakefield Electron Acceleration where longer wavelengths expectedly will engender a proportional improvement in the beam's charge and emittance;
- IFELs with more than 1 GeV/m acceleration gradients;
- Vacuum Electron Acceleration that will acquire a new spin; combining this with Compton probing will reveal the much sought, but still elusive multiplication of electron energy within the laser's focus;
- New opportunities in the development of radiation sources:
 - Generating a continuum in high Compton harmonics in the x-ray and gamma-ray regions.
 - Extending HHG super-continuum in gases to 8 keV (up to the 80,000th harmonic).
 - Realizing intense THz radiation upon the production of hot electrons from focusing the laser on foils.

We will capitalize upon such opportunities for new scientific outreaches at different stages of the CO₂ laser upgrade, as illustrated in **Figure 12**.

The six scientific cases, discussed below, exemplify the new opportunities for user experiments that will benefit from the future 100 TW CO₂ laser. Three of them (Shock Wave Ion Acceleration, LWFA, and IFEL) belong to the field of advanced particle accelerators, and the other three (Inverse Compton harmonic continuum, THz source, and HHG super-continuum) to advanced radiation sources. We review these applications in the following paragraphs.

Proton accelerator (from 2 MeV to 200 MeV)

One of main arguments for developing multi-terawatt CO₂ laser technology is to empower research on ion acceleration towards laser-driven ion sources for radiation therapy of cancers. The method of Laser Shock Wave Acceleration (LSWA), recently demonstrated with the CO₂ laser and discussed in detail in Appendix B, holds strong promise for becoming one of the leading candidates to achieve the ultimate goal of attaining 200 MeV proton beams with parameters suitable for medical treatment. The major distinctive features of this methodology include the production of monoenergetic ion-beams, and the close-to-linear scaling of ion energy with the laser's intensity. This accomplishment allows us to project that the 200 MeV goal can be met at $\sim 10^{18}$ W/cm² of the CO₂ laser intensity, attainable at 100 TW peak power. Recent simulations shown in **Figure 13** support these arguments.

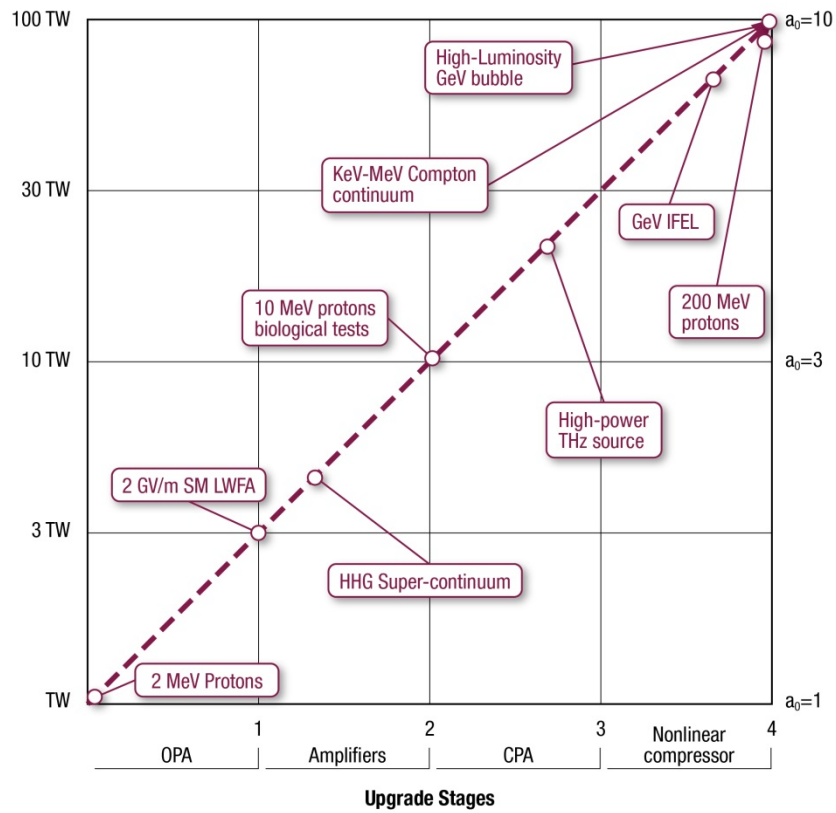


Figure 12. Opportunities for new science outreach at different stages of upgrading the CO₂ laser.

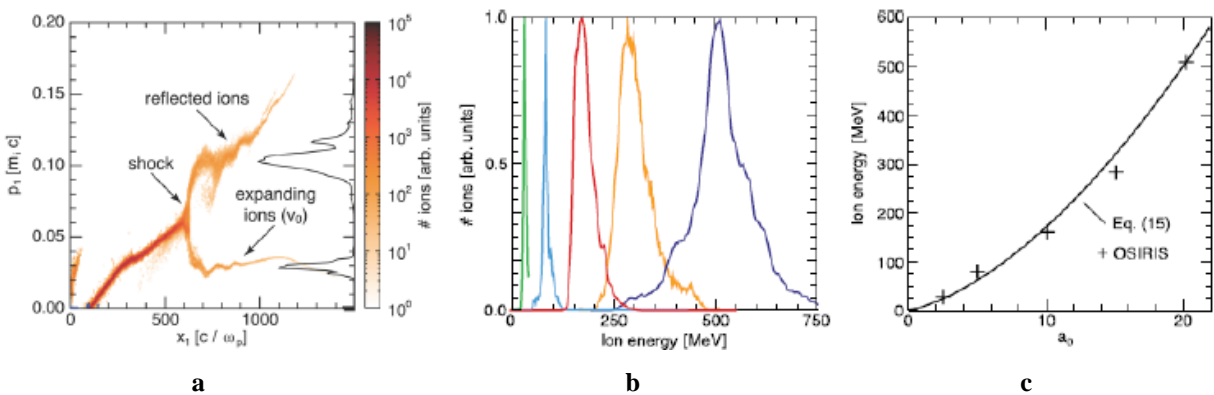


Figure 13. Shock-wave simulations (a), ion spectra at different laser a_0 with red corresponding to $a_0=10$ (b), and dependence of maximum proton energy on a_0 (c).

Even if we can produce plasma targets compatible with 1- μm laser sources (required density $\geq 10^{21} \text{ cm}^{-3}$), intensity a hundred times higher would be required to reach the same shock-wave

velocity. Recent findings support the notion that a collisionless shock wave, which is the ultimate source of proton beams, exists only in the course of the laser pulse. Therefore, in addition to the peak power that defines the immediate velocity of the shock wave, attaining a pulse of picosecond duration is critically important to allow the shock wave to fully penetrate a typical gas-jet target of about 0.5 mm thick. Typically, at several tens of femtoseconds, it is unlikely that ultra-fast solid-state lasers could be suitable in practice for the LSWA task. This makes the prospective ultra-fast 100 TW CO₂ laser the prime candidate for achieving this promising method of producing ion beams for cancer therapy.

Prospects for high-luminosity LWFA

Laser wakefield accelerators (LWFAs), wherein a high-intensity laser pulse creates a plasma wake that can accelerate electrons, have demonstrated very high acceleration gradients up to 100 GV/m. Most experiments used near-infrared laser sources ($\lambda=0.8\text{-}1\ \mu\text{m}$) that offer multi-terawatt peak-powers and femtosecond pulses. It was noticed here that longer laser wavelengths have certain advantages due to the wavelength scaling in the electrons' ponderomotive potential that is crucial in launching collective plasma-electron motion and wakes. These advantages have not been fully explored experimentally because of the lack of long-wavelength multi-TW mid-IR laser sources with a pulse length sufficiently short to drive a plasma wake at a competitively high field-gradient.

The parameters achievable with the ATF CO₂ laser provide the first-time possibility to perform LWFA experiments at 10 μm . In addition, the ATF has been undertaking capillary-discharge experiments wherein we demonstrated channeling of the CO₂ laser light. Thus, the ATF not only possesses a viable laser driver for LWFA, but also a verified means to confine it over many Rayleigh lengths.

The so-called resonant LWFA normally requires the length of the laser pulse, τ to be comparable to or less than half of the plasma wake's period, π/ω_p , where $\omega_p \propto n_e^{1/2}$. At the plasma density of $n_e=10^{16}\ \text{cm}^{-3}$, considered close to the low limit for a meaningful high-gradient LWFA, this corresponds to $\tau \approx 0.4\ \text{ps}$. An amplified 2-ps CO₂ laser pulse, soon to be attained with the implementation of OPA as a front end for the upgraded ATF CO₂ laser, would be still too long for optimally generating a plasma wake in the resonant LWFA.

However, simulations show that even though the 2-ps duration of the laser pulse is several times longer than that for "resonant" LWFA, a very strong wake still can be generated. This achievement reflects the nonlinear evolution of the laser pulse upon coupling with the plasma. The laser pulse's envelope (**Figure 14a**) becomes modulated, with the peak intensity more than 50% higher than its initial value. However, a more important effect, in terms of wake generation, is the nonlinear steepening of the pulse, caused by two effects: Self-focusing at the peak of the laser pulse; and modulation growing near the pulse's trailing edge. Such a modulated pulse falls into resonance with the plasma, so producing a strong wake.

Simulations predict a wake amplitude $>1\ \text{GV/m}$ for a 2-ps, 2.5-TW laser pulse. In addition, the wake is very regular, as illustrated in **Figure 14b**. The formation of regular wakes is one vital prerequisite for staging LWFA devices in series, a feature that will be important eventually for developing practical accelerators based upon LWFA. We plan to probe the accelerating gradient with a femtosecond electron bunch from the ATF linac.

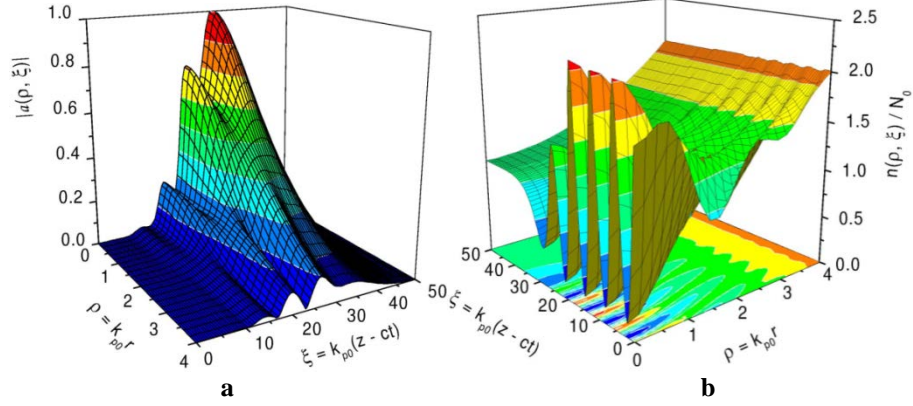


Figure 14. The normalized laser field (a), and electron plasma density (b), after 6.7 cm propagation in plasma.

These would be the first experiments to demonstrate LWFA in a linear regime over an extended interaction length using capillary discharge plasma for channeling the laser. Although not record-breaking in comparison with Ti:Sapphire-driven LWFA, the ATF experiment should demonstrate good acceleration gradients exceeding those of conventional RF accelerators by an order-of- magnitude, even *at relatively low 2.5 TW CO₂ laser power*. This experiment will become a test bed for exploring seed-bunch phasing into the wake, and beam-loading effects.

The LWFA experiment at the ATF will progress together with the laser power upgrade, finally reaching the condition for the bubble LWFA regime at the following CO₂ laser parameters:

Laser peak power	$P = 100 \text{ TW}$
Laser pulse duration	$\tau = 500 \text{ fs}$
Laser pulse energy	$E_L = 50 \text{ J}$

We have taken the following considerations into account for attaining the bubble regime:

The laser power should exceed the threshold value for the blow-out regime:

$$P > P_{bubble} \cong P_{rel}(\omega_0\tau)^2 \cong (\tau[\text{fs}] / \lambda[\mu\text{m}])^2 \times 30 \text{ GW}, \quad (1)$$

where $P_{rel} = m^2 c^5 / e^2 \approx 8.5 \text{ GW}$, $\omega_0\tau = 2\pi c\tau / \lambda \cong 1.9\tau[\text{fs}] / \lambda[\mu\text{m}]$.

For these laser parameters above, $P_{bubble} \cong 75 \text{ TW}$ is just slightly below the laser's power at the laser pulse duration $\tau = 500 \text{ fs}$.

There are additional key conditions for the bubble regime:

The radius of the laser pulse, R , should scale as

$$k_0 R \cong \left(\frac{n_{cr}}{n_e} a_0 \right)^{1/2}, \quad (2)$$

and its duration should be short compared with its radial size.

$$\tau \leq R/c, \quad \tau \leq \frac{\lambda}{2\pi c} \left(\frac{n_{cr}}{n_e} a_0 \right)^{1/2}. \quad (3)$$

These conditions determine the range of plasma density and intensity, that for $a_0 = 8$ gives

$$n_e \cong 5 \times 10^{15} \text{ cm}^{-3}$$

$$R \cong 150 \mu\text{m},$$

and the length of acceleration

$$L_{acc} \cong 0.7 \frac{c\tau}{\lambda} Z_R \approx 8 \text{ cm}. \quad (4)$$

The energy of the quasi-monoenergetic peak in the spectrum of accelerated electrons is

$$E_{mono} \approx 0.65 mc^2 \left(\frac{P}{P_{rel}} \right)^{1/2} \frac{c\tau}{\lambda} \approx 600 \text{ MeV}. \quad (5)$$

The prospective parameters of the bubble electron accelerator are compared in **Table 3** to the 2-GeV accelerator recently demonstrated with a Petawatt Texas laser.

Moreover, a relatively low plasma density, in combination with bigger laser spots, both features typical for a CO₂ laser-driven LWFA, open up the possibility for increasing the size and charge of the electron bunch.

The number of accelerated electrons in the monoenergetic peak is

$$N_{mono} \approx \frac{1.8}{k_0 r_e} \left(\frac{P}{P_{rel}} \right)^{1/2} \approx 10^{11} \quad (6)$$

which is about 16 nC (!). A bubble a thousand fold bigger in volume (in proportion to the plasma wavelength) will relieve the problem of space charge and simplify electron injection into the acceleration stages.

Table 3. Comparative parameters for bubble accelerator driven with 1 μm - and 10- μm lasers.

λ	1 μm	10 μm
P	1.1 PW	100 TW
a_0	8	8
τ	170 fs	500 fs
n_e	$5 \times 10^{17} \text{ cm}^{-3}$	$5 \times 10^{15} \text{ cm}^{-3}$
P_{bubble}	0.9 PW	75 TW
P_{cr}	43 TW	43 TW
L_{ph}	20 cm	200 cm
L_{PD}	10 cm	30 cm
E_{max}	2 GeV/cm	0.2 GeV/cm
L_a	1 cm	3 cm

These features, in combination with the available femtosecond electron injector, make the ATF's LWFA experiment a viable complement to the LWFA research ongoing at other PW-class laser facilities. We will apply the experimental experience gained during our optimizing bunch injection into the initial low-power linear LWFA experiment to quickly assess conditions for a

high-luminosity bubble accelerator. The parameters for phasing consecutive accelerating stages also will be investigated. The experiment will provide a platform for directly comparing different methods of electron seeding into the bubble, such as via a conventionally produced electron bunch from a linac, or an all-optical method with direct photoionization from an external Ti:Sapphire laser that will become available at the ATF according to the upgrade plan.

Overall, the ATF upgrade will provide unprecedented opportunities for the cost-effective, comprehensive study of a spectrum of scientific- and technological-approaches essential for developing plasma-based, high-gradient, multi-stage accelerators in our advances towards prospective TeV-class electron-positron colliders.

1-GeV IFEL

Recently, a UCLA group headed by PI – Pietro Musumeci carried out a milestone IFEL experiment at the ATF. The experiment completed its first run with the successful demonstration of 100 MV/m energy gradient in a 54-cm helical undulator, dramatically doubling the beam’s energy from 50-MeV to 105-MeV. These numbers set a record in IFEL acceleration and naturally call for follow-up experiments to extend the energy reach of the scheme, and to improve the quality of the output beam. The 100 TW CO₂ laser upgrade will assure that the ATF is the ideal place to continue IFEL research. According to the UCLA’s letter of intent, a new, strongly tapered, helical undulator will support accelerating a 50-MeV beam to more than 1.2 GeV in 1 m with an rms energy spread < 1%, so attaining a new world-record energy gain (>1 GeV) and gradient (>1 GV/m) for a vacuum-laser accelerator. **Table 4** lists the parameters of the proposed 1-GeV IFEL experiment.

Table 4. Parameters for BNL’s high-gradient, high-energy-gain IFEL experiment

Input beam energy	50 MeV
Laser wavelength	10.3 μm
Laser seed power	100 TW
Laser Rayleigh range	25 cm
Undulator wavelength (initial-final)	4 cm – 20 cm
Final beam energy	1200 MeV
Average accelerating gradient	>1 GV/m
Laser size (at focus)	950 μm
Undulator length	100 cm
Undulator peak field (initial-final)	0.6 – 1.2 T

As demonstrated in RUBICON, tapering will be achieved by choosing magnets of different thicknesses for each period of the undulator. The amplitude of the magnetic field can be adjusted and tuned by inserting or extracting the magnets. The undulator gap should be larger than 10 mm to allow the full unhampered transmission of the laser. Due to extreme tapering, the number of periods is relatively small (8 full periods), with the last two accounting for a large portion of energy gain. This geometry is important as it allows us to use ultrashort laser pulses (<0.5 ps), so avoiding the degradation of the interaction due to slippage. Motorized mechanical tuning of the last magnets could enable online fine tuning of the accelerator characteristics, such as output energy, energy spread, and the angle of the output trajectory.

The letter of intent from Prof. Musumeci is concluded with his statement that “Relatively long CO₂ wavelength has significant advantages due to relaxed tolerances in alignment and synchronization.”

THz Radiation Source

Different physical mechanisms are being explored with the goal of accessing high-power THz radiation sources desirable for different emerging applications ranging from material studies to work for Home Land Security. Arguably the most powerful sources of such radiation are based on collective motion of electrical charges induced by an intense laser.

Efficient energy conversion from a laser beam to THz radiation recently was reported as a byproduct of TNSA ion acceleration experiments wherein a laser was focused onto a thin foil. Hot electrons escape the laser focus at several MeV energies; then they are stopped by the positive charge of the foil. This violent change of the electron's energy at the picosecond time-scale produces single-cycle THz radiation that can be collected and collimated by a coin-sized parabolic mirror focused at the rare surface of the foil.

CO₂ lasers are well-known for their high efficiency in producing hot electrons. Indeed, as the ponderomotive energy of the electrons escaping the laser focus scales as $\Phi = I/4\omega^2$, a hundred times higher intensity is required from a 1- μm laser to induce the same electron energy as does the long-wavelength CO₂ laser. This wavelength scaling was demonstrated at the ATF where only 10^{16} W/cm² of the CO₂ laser intensity was required to produce the same ion acceleration via the TNSA mechanism as was 10^{18} W/cm² by a solid state laser used elsewhere.

Furthermore, $\lambda=1$ μm permits up to a tenfold tighter focus at the diffraction limit. This way, the same ponderomotive electron energy can be realized with a 1- μm laser of the same peak power as a CO₂ laser, but notably, in a hundredfold smaller surface area; this results in a corresponding drop in the integral hot-electron yield. Therefore, we can safely predict that a 100 TW CO₂ laser could be 100 times more efficient in producing hot electrons compared with a 100-TW solid-state laser. In other words, a 10-PW solid-state laser will be required to match the 100 TW CO₂ laser in the production rates of hot-electrons and THz radiation. Considering that up to 50% of the CO₂ laser's energy can be routed into generating hot electrons, and that a considerable portion of these electrons end up forming a rear-surface sheaf layer whilst radiating THz photons in the process, we can predict that the proposed method may become the most energy-efficient source of single-cycle THz radiation. The ATF holds a unique position for facilitating such research that is a natural continuation of our successful TNSA ion- acceleration studies, and might well culminate in a record-breaking demonstration of a high-intensity THz source upon our further upgrade of laser power.

Importantly, the THz radiation process has a low laser-intensity threshold and can be studied with the already available 1 TW ATF CO₂ laser. After the laser upgrade, the ATF will acquire the capability to configure a high-repetition (10-100 Hz) CO₂ laser system with up to 10 TW peak power that is highly meaningful as a practical source of high-power THz radiation for a plethora of applications.

HHG super-continuum

High-harmonic generation (HHG) is another advanced broad-band source of radiation that covers the EUV and x-ray regions. HHG radiation consists of femtosecond-to-attosecond duration pulses with full spatial coherence; accordingly, this makes it very attractive for a

spectrum of applications, including tracking the dynamics of electrons in atoms, molecules, and materials. Ultrashort x-ray pulses can capture the coupled motions of charges, spins, atoms, and phonons by monitoring changes in absorption or reflection that occur as the state or shape of a material or a molecule changes.

HHG begins with tunnel ionization of an atom in a strong laser field. The electron that escapes the atom is accelerated by the laser's electric field and, when driven back to its parent ion by the laser, can coherently convert its kinetic energy into a high-harmonic photon. The highest energy HHG photon emitted is given by $h\nu_{cutoff} = I_p + 3.17\Phi$, where I_p is the ionization potential of the gas, and $\Phi = I/4\omega^2$, is the quiver energy of the liberated electron in a laser field.

Generating bright, fully coherent HHG beams requires macroscopic phase matching, wherein the laser and high-order nonlinear polarization propagate in phase (at the speed of light) throughout a medium to ensure that the HHG light emitted from many atoms is combined coherently. Phase matching is achieved by balancing the neutral gas and free-electron plasma dispersion experienced by the laser; it is possible only up to some critical ionization level that depends on the gas species and laser's wavelength. Because ionization rises with laser intensity, the critical ionization limits the highest photon energy for which phase matching can be implemented. Recent work explored the wavelength dependence of the HHG yield, which scales as $h\nu_{cutoff} \propto \lambda^{1.7}$. This scaling was verified in a series of experiments starting with Ti:Sapphire lasers operating at a 0.8- μm wavelength with <150 eV EUV photons produced, then extending the continuum to >0.5 keV using 2- μm lasers, and finally to 1.6 keV with a 3.9- μm laser. Using a picosecond CO₂ laser promises to push the x-ray plateau to 8.5 keV, corresponding to the 80,000th order of the CO₂ harmonics!

We can initiate a meaningful demonstration of a record-broad x-ray super-continuum with our existing 1 TW CO₂ laser.

Upon the planned laser upgrade, components operating at a high repetition rate (10 Hz and potentially higher) will be added, so allowing us to reconfigure the system to 10- TW operation at the same repetition rate, thereby making the proposed attosecond coherent x-ray source invaluable for practical applications.

Compton super-continuum

Laser synchrotron sources (LSS) based on inverse Compton scattering (ICS) complement conventional synchrotron light sources via attaining a hard x-ray region with a relatively compact electron accelerator while producing orders-of-magnitude higher peak brightness per single shot. These advantages were experimentally exploited in the linear regime of laser intensities $a_0 < 1$, where $a_0^2 = 3.7 \times 10^{-19} I \lambda^2$ for I in Watts/cm² and λ in μm .

CO₂ lasers facilitate our achieving high x-ray ICS yields by delivering 10 times more photons per Joule of laser energy compared with 1- μm lasers. Another contributing factor for LSS application of CO₂ lasers is their relatively mild diffraction-limited focus that is well coordinated with the e-beam's size under the practically meaningful compact-focusing configuration.

We address here the second avenue, still experimentally unexploited, to shorter ICS wavelengths attained without the energy increase of compact linear accelerators. This approach is based on the harmonic frequency up-shift. For $a_0 \gg 1$, numerous harmonics are generated, yielding a continuum of scattered x-ray radiation with harmonics increasing in intensity as $(\omega/\omega_1)^{2/3}$ out to some critical harmonic number n_c ; beyond this, the intensity of the scattered radiation

exponentially decreases. This number is $n_c \cong 3a_0^2/4$ for linear polarization, and $n_c \cong 3a_0^2/2\sqrt{2}$ for circular polarization. This number is close or exceeds 1000 for $a_0=10$ aimed at the ATF CO₂ laser upgrade. However, this does not mean that the 6-keV x-rays, observed at the ATF when a CO₂ laser collided with a 60-MeV e-beam in the linear regime, will be converted into the MeV gamma-region. The fundamental ICS frequency $\omega_1 \approx \omega_0 \frac{4\gamma^2}{1+a_0^2/2}$ simultaneously drops nearly a hundredfold due to the mass shift $\bar{m} = m\sqrt{1+a_0^2}$. Still, the MeV gamma-region might well be attained upon the ATF's linac optional upgrade to 500 MeV.

An LSS, based on the nonlinear Thomson scattering of intense CO₂ laser from the electron beam has several potentially unique and attractive features that may serve a variety of x-ray spectroscopic and imaging applications. These features include compactness, relatively low cost, tunability, narrow bandwidth, short-pulse structure, high-photon-energy operation, well-collimated photon beams, polarization control, and high levels of photon flux and brightness.

In addition, for sufficiently cold-electron distributions, we can generate short-wavelength radiation by the stimulated (coherent) backscattering of intense lasers from beams and plasmas. Stimulated backscattered harmonic generation may afford us a method for producing coherent x rays via a laser-pumped free-electron laser.

In completing this example, we would again confirm and highlight the unique opportunities for research offered at the ATF by the combination of a high-brightness e-beam and the $a_0=10$ 10- μ m laser. As discussed earlier, the efficiency of the laser/e-beam interaction crucially depends upon the spatial- and temporal- overlap between both beams. Both conditions are quite well satisfied with picosecond CO₂ laser pulses focused to several- λ 's focal spots. This is a situation wherein the tighter focusing ability of shorter-wavelength lasers does not help and, accordingly, a 100 times more powerful 1- μ m laser will be required to explore the effect to the same a_0 and harmonic number as a 10- μ m laser. As the only facility worldwide combining a high-brightness e-beam with the $a_0=10$ laser, the ATF will hold an exclusive position for leading this cutting-edge research in highly nonlinear Compton scattering, a field that is equally important for fundamental- and applied- physical sciences.

Suggested Reading

1. ATF CO₂ laser: *Optics Express* **19**, 7717 (2011)
2. Femtosecond pulse compression: *Quantum Electronics* **39**, 663 (2009)
3. Ion acceleration: *PRL* **106**, 014801 (2011); *Phys. Plasmas* **20**, 056304 (2013)
4. LWFA: *Nature Communication* **4**, 1988 (2013)
5. IFEL: *PRST AB* **15**, 061301 (2012)
6. HHG: *Science* **336** 1287 (2012)
7. THz: *New Journal of Physics* **14**, 083012 (2012)
8. Nonlinear ICS: *Phys. Rev.* **E 48**, 23003 (1993)